GLOBAL WARMING POTENTIAL OF CARBONATION/CHLORIDE EXPOSED CONCRETE WITH(OUT) CONSIDERATION OF THE PROPAGATION PERIOD IN SERVICE LIFE ASSESSMENT

Philip Van den Heede [(1)] *, Renée Callens [(1)] and Nele de Belie [(1)]

(1) Magnel Laboratory for Concrete Research, Ghent University, Belgium

* philip.vandenheede@ugent.be

Abstract

When studying concrete's susceptibility to carbonation-/chloride-induced corrosion, the focus is usually on the corrosion initiation period. Service life prediction performed as such only quantifies the time to depassivation of the reinforcing steel and does not involve any damage. As a consequence, the actual service life is underestimated. In this paper, it has been evaluated whether the time between steel depassivation and unacceptable corrosion-induced cracking is significant or not. This information is important because it affects the expected number of rehabilitation actions with time and therefore also the sustainability of a concrete composition. Service life calculations done in compliance with the well-known DuraCrete models imply that the propagation period cannot be neglected in a carbonation exposed environment (exposure class XC3), especially for concrete with supplementary cementitious materials such as fly ash and silica fume (propagation period > 100 years). On the other hand, the propagation period was observed to be very short (max. 8.7 years) in a chloride exposed environment (exposure class XS2). Logically, the differences in global warming potential for not considering the propagation period were mainly important in presence of carbonation. In exposure class XS2, the sole consideration of the initiation period can be acceptable.

1. INTRODUCTION

To quantify the possible reduction in greenhouse gas emissions for concrete with high cement replacement levels in an adequate way, it is of importance to consider the differences in strength and durability with traditional concrete in the environmental study. So far, several attempts have been made to calculate a global warming potential (GWP) for concrete with high volumes of fly ash (FA) by choosing strength and service life related functional units for life cycle assessment (LCA). This has been done both for carbonation and chloride exposed environments [1]. However, the underlying service life assessment in these studies only comprised the corrosion initiation period. It remains for the moment unknown whether neglecting the propagation period can lead to a significant underestimation of the actual service life as well as to an overestimation of the concrete's GWP. Therefore, the duration of

the corrosion propagation period was evaluated in accordance with the DuraCrete model [2]. It requires mainly the bulk resistivity of concrete as experimental input. This concrete property has been determined for four different concrete compositions. The environmental effects of having different propagation periods were studied by following a typical four-step LCA methodology in the software SimaPro.

2. MATERIAL CHARACTERISATION

2.1 Concrete mixtures

In total, four concrete mixtures were manufactured (Table 1). Mixture T(0.55) is an Ordinary Portland Cement (OPC) concrete composition with a minimum cement content and a maximum water-to-cement (W/C) ratio conforming to NBN B15-001 for exposure class XC3. This exposure class corresponds with a moderately humid environment with exposure to carbonation-induced steel corrosion. A common example of such an environment is exterior concrete sheltered from rain. On the other hand, the total cement content and W/C ratio of mixture T(0.45) meet the criteria of NBN B15-001 to make the concrete quantifiable for use in exposure class XS2. In other words, it counts as a proper reference in environments where concrete is permanently submerged in seawater.

Table 1: Concrete mixture proportions

	T(0.55)	T(0.45)	F50	F40SF10
Sand 0/4 (kg/m³)	715	715	645	791
Aggregate 2/8 (kg/m³)	516	515	465	687
Aggregate 8/16 (kg/m³)	672	671	606	454
CEM I 52.5 N (kg/m³)	300	340	225	170
Fly ash (FA) (kg/m³)	0	0	225	136
Silica fume (SF) (kg/m³)	0	0	0	34
Water (kg/m³)	165	153	157.5	119
Superplasticizer (ml/kg B)	2 (b_1, b_2)	4 (b_1)	5 (b_1, b_2)	14 (b_1), 12 (b_2)
W/B	0.55	0.45	0.35	0.35
FA/B	0	0	50	40
SF/B	0	0	0	10
Slump*	S3 (b_1), S4 (b_2)	S3 (b_1)	S3 (b_1), S5 (b_2)	S4 (b_1, b_2)
Strength class**	C35/45 (b_1) C30/37 (b_2)	C50/60 (b_1)	C40/50 (b_1, b_2)	C50/60 (b_1, b_2)

* S1 (10-40 mm), S2 (50-90 mm), S3 (100-150 mm), S4 (160-210), S5 (≥ 220 mm)

** based on the 5% characteristic (compressive strength) value cf. EN 1990 (n = 4 (b_1), 3 (b_2), V_X: unknown)

Within the other two concrete compositions 50% of the total binder (B) content consisted of supplementary cementitious materials. Mixture F50 counts as a High-Volume Fly Ash (HVFA) composition since half of the total binder content consisted of pozzolanic FA. To compensate for the rather slow FA hydration reaction, a higher total binder content of 450 kg/m² and a lower water-to-binder (W/B) ratio (0.35) was applied in this composition. As such, quite a high early age strength performance could still be achieved. The strength class of the material (= C40/50), which is based on the 28-day characteristic compressive strength,

proves this. To improve the early age strength performance without increasing the total binder content too much, silica fume (SF) could be introduced as third powder in the binder system. This was done for composition F40SF10 in which the total binder content consisted for 50% of Portland cement, 40% of FA and 10% of SF. With a total binder content of only 340 kg/m³, a strength class of no less than C50/60 could still be achieved.

Note that two batches of concrete were made for all compositions except T(0.45). Chloride migration coefficients, tensile splitting strengths and resistivities were determined on samples from the first batch (b_1). The specimens from the second batch (b_2) were used for the accelerated carbonation experiments.

2.2 Carbonation testing

After 21 days of optimal curing at 20°C and 95% RH, 5 of the 6 surfaces of 9 cubic specimens (side: 100 mm) per mixture were treated with an impermeable coating to ensure a unidirectional flow of CO_2 during an accelerated carbonation experiment. The untreated side was always a cast surface of the cube. After applying the coating, the specimens were stored again under optimal curing conditions until they were 28 days of age. Then, the cubes of mixtures T(0.55), F50 and F40SF10 were stored in carbonation chamber conditioned at 1% CO_2, 20°C and 60% RH. Every four weeks, three cubes per test series were taken out of the chamber and split. After spraying the 1% phenolphtalein solution onto the fractured surfaces, the carbonated area showed colourless, while the non-carbonated area coloured purple. For each concrete mixture tested, the measured carbonation depths x (in mm) were plotted as a function of the square root of the exposure time t (in weeks) to determine an experimental (accelerated) carbonation coefficient $A_{1\%}$ (in mm/√weeks). Because the DuraCrete prediction model for carbonation-induced corrosion uses data from a carbonation experiment at 2% CO_2 [3], our data still needed to be converted in order to be representative for the latter CO_2 concentration. Therefore, the formula proposed by Sisomphon and Franke [4] was used (Equation 1). It allows for converting carbonation coefficients obtained at a certain CO_2 concentration to a carbonation coefficient representing another concentration. The formula is believed to be valid for CO_2 concentrations up to 3% [4].

$$\frac{A_{2\%}}{A_{1\%}} = \frac{\sqrt{c_{2\%}}}{\sqrt{c_{1\%}}} \tag{1}$$

Once a theoretical carbonation coefficient for 2% CO_2 was obtained as such, the well-known square-root-time law was applied again to calculate the theoretical carbonation depth d_c (m) after 28 days of exposure in an atmosphere containing 2% CO_2. The latter value is the basic input parameter to the DuraCrete model for estimating the time to carbonation-induced steel depassivation [3]. It enables the calculation of the 5% characteristic inverse effective carbonation resistance $R_{carb,0}^{-1}$ in $m^2/s/kg_{CO2}/m^3$ (Equation 2).

$$R_{Carb,0}^{-1} = \left(\frac{d_c}{419.45} \right)^2 \tag{2}$$

2.3 Chloride migration testing

The resistance to chloride penetration was evaluated experimentally using the rapid chloride migration test as described in NT Build 492 [5]. This method enables the calculation

of a non-steady state chloride migration coefficient D_{nssm} ($\times 10^{-12}$ m²/s) after 28 days of optimal curing at 20°C and 95% RH. Given the mean value, the standard deviation on the individual values and the number of tested samples (n = 6), a 5% characteristic value can be calculated for the chloride migration coefficient. By converting the characteristic D_{nssm} values to mm²/years and subsequently taking the inverse of the latter, a new parameter is obtained which counts as the characteristic chloride resistance $R_{cl,0}^{c}$ which can be used for estimating the time to chloride-induced steel depassivation (Section 3.2).

2.4 Resistivity measurements

The electrolytic resistivity ρ_0^c of the concrete is an experimental input parameter to the model for estimating the time to unacceptable corrosion-induced cracking. Per studied concrete composition this property should be determined by means of a standardized test method. As recommended in DuraCrete [3], the Two-Electrode Method (TEM) was used for this purpose. The bulk resistivity ρ_{TEM} was determined with a commercially available Proceq Resipod resistivity meter on six concrete cylinders (H: 50 mm, Ø: 100 mm) per concrete mixture. The samples were not water cured for 28 days to avoid a leaching of ions which can substantially affect the recorded value of the resistivity [7]. Instead, they were vacuum saturated after 28 days of optimal curing at 20°C and 95% RH in accordance with NT Build 492 [5]. The vacuum saturation step just before the resistivity measurements was included to ensure thoroughly wet specimens with exclusion of very pronounced leaching phenomena. The characteristic value of the potential electrolytic resisitivity ρ_0^c in Ωm corresponds with the 5% fractile of the predicted (normal) distribution of the performed measurements.

2.5 Tensile splitting strength

NBN EN 12390-6 indicates that the tensile splitting strength of concrete can be determined on samples with varying geometries. The standard sample geometry is a concrete cylinder. However, cubic or prismatic specimens could be used as well. DuraCrete does not really specify which sample geometry should be used for quantifying $f_{c,sp}^{d}$ [3]. In this research, prismatic specimens (300 × 150 × 150 mm³) were used. The fracture plane was parallel to the casting direction. In accordance with DuraCrete [2], the 5% characteristic 28-day tensile splitting strength was adopted as design value $f_{c,sp}^{d}$ in the prediction model for estimating the time to unacceptable corrosion-induced cracking.

3. SERVICE LIFE PREDICTION

3.1 Time to carbonation-induced steel depassivation

In the DuraCrete guideline for durability design [2], a semi-probabilistic design equation is given for carbonation-induced steel depassivation (Equation 3).

$$g = (d - \Delta d) - \sqrt{\frac{2 \cdot c_{s,ca}^{d} \cdot t}{R_{ca}^{d}}} \tag{3}$$

With d, the concrete cover (XC3: 35 mm), Δd, safety margin for the concrete cover (= 14 mm), $c_{s,ca}^{d}$, design value of the surface concentration (= 5.0×10^{-4} kg/m³), t, time (years), R_{ca}^{d}, design value of the carbonation resistance (year · kg/m³/mm²). The value of the latter parameter can be calculated from Equation 4.

$$R_{ca}^{d} = \frac{R_{0,ca}^{c}}{k_{e,ca}^{c} \cdot k_{c,ca}^{c} \left(\frac{t_0}{t} \right)^{2n_{ca}^{c}} \cdot \gamma_{R_{ca}}} \tag{4}$$

With $R_{0,ca}^{c}$, the characteristic value of the carbonation resistance that results from the accelerated carbonation test (= $1/R_{carb,0}^{-1}$ in year · kg/m³/mm², see Section 2.2), $k_{e,ca}^{c}$, the characteristic value of the environment factor (= 0.86), $k_{c,ca}^{c}$, the characteristic value of the curing factor (= 0.76), t_0, time of reference at which the carbonation experiment is performed (= 28 days or 0.0767 years), n_{ca}^{c}, characteristic value of the age factor (= 0.098), γ_{Rca}, a partial factor with respect to the carbonation resistance (= 2.10).

Note that the values mentioned here for $k_{e,ca}^{c}$ and n_{ca}^{c} are normally valid for OPC concrete [2]. No values are given for HVFA and FA+SF concrete. In literature, little or no additional information could be found on the actual value of their age factors as calculated cf. the Duracrete model. True, Burden [6] describes some sort of a general age factor of 0.25 in his ageing related carbonation rate model. However, as Burden's model relies on several other fitted parameters as well, it is not immediately implementable in Equation 4 and thus 0.25 cannot be used as a proper value for n_{ca}^{c}. More research on this matter is thus still needed. Evidently, the output of the DuraCrete model should be updated once more mix specific information on n_{ca}^{c} becomes available. The same goes for $k_{e,ca}^{c}$.

3.2 Time to chloride-induced steel depassivation

DuraCrete also provides a semi-probabilistic design equation stating that corrosion is initiated when the chloride concentration around the reinforcement exceeds the critical chloride threshold value for onset of active corrosion (Equation 5) [2].

$$g = c_{cr}^{c} \cdot \frac{1}{\gamma_{cr}} - A_{Cs,cl} \cdot (w/b) \cdot \gamma_{cs,cl} \cdot \left[1 - \operatorname{erf}\left(\frac{d - \Delta d}{2\sqrt{\frac{t}{R_{cl}^{d}(t)}}} \right) \right] \tag{5}$$

With c_{cr}^{c}, the characteristic value of the critical chloride concentration (= 1.9 m%/binder), γ_{cr}, a partial factor for the critical chloride concentration (= 1.06), $A_{Cs,cl}$, a regression parameter (OPC: 10.3, FA: 10.8, SF: 12.5) describing the relation between the chloride surface concentration and the W/B ratio (T(0.45): 0.45, F50: 0.35, F40SF10: 0.35), $\gamma_{Cs,cl}$, a partial factor for the chloride surface concentration (= 1.40), d, the concrete cover (XS2: 50 mm), Δd, safety margin for the concrete cover (= 14 mm) and R_{cl}^{d}, design value of the chloride resistance which can be calculated using Equation 6.

$$R_{cl}^{d}(t) = \frac{R_{cl,0}^{c}}{k_{e,cl}^{c} \cdot k_{c,cl}^{c} \cdot \left(\frac{t_0}{t} \right)^{n_{Cl}^{c}} \cdot \gamma_{Rcl}} \tag{6}$$

With $R_{cl,0}^{c}$, characteristic value of the chloride resistance as calculated from the non-steady-state chloride migration coefficients (see Section 2.3), $k_{e,cl}^{c}$, characteristic value of the environment factor (= 1.32), $k_{c,cl}^{c}$, characteristic value of the curing factor (= 0.79), t_0, time of

reference at which the non-steady state migration experiment is performed (= 28 days or 0.0767 years), t, time in years, n_{Cl}^{c} characteristic value of the age factor (OPC: 0.30, FA: 0.69, SF: 0.62), γ_{RCl}, a partial factor for the chloride resistance (= 2.35).

It should be noted that the value mentioned for the critical chloride concentration c_{cr}^{c} is an interpolated value for submerged OPC concrete with a W/C ratio of 0.45. DuraCrete mentions an increase in critical chloride concentration with a decrease in W/C ratio. No specific values are included in the DuraCrete model code for concrete in which the binder system partially consists of FA (and SF) [2]. Therefore, the c_{cr}^{c} value for OPC concrete was adopted for compositions F50 and F40SF10 as well. True, the fact that the W/B ratio (= 0.35) of these mixtures was considerably lower than the W/C ratio of the OPC reference, may indicate that the critical chloride concentrations for these mixtures can be higher than 1.9 m%/binder. However, this possible extra advantage inherent to lowering the W/B ratio is not taken into account for now because the actual value for HVFA and FA+SF concrete has not been verified yet experimentally.

The above mentioned value for $k_{e,cl}^{c}$ is normally also just valid for submerged OPC concrete. Due to a lack of values for binder systems containing considerable portions of FA (and SF), the same $k_{e,cl}^{c}$ value was used for compositions F50 and F40SF10.

3.3 Time to unacceptable corrosion-induced cracking

The semi-probabilistic limit state function for the corrosion propagation period suggested by DuraCrete enables an estimation of the time to unacceptable corrosion-induced cracking of the concrete cover on top of the rebar. This unacceptable cracking is associated with a critical crack width of 1.0 mm which normally marks the onset of concrete spalling [2]. Equation 7 represents the as such defined limit state function in its most basic form.

$$g(x) = w_{cr} - \left(w_0 + b^{c} \cdot \gamma_b \cdot \left(p^{d} - p_0^{d}\right)\right) \tag{7}$$

With w_{cr}, the critical crack width of 1.0 mm, w_0, the width of the initial visible crack (= 0.050 mm), b^{c}, the characteristic value of the parameter accounting for the position of the rebar (= 0.0104 mm/µm), γ_b, partial factor for b^{c} in case of a normal cost of mitigation of risk relative to the cost of repair (XC3: 1.40, XS2: 1.0), p^{d}, the design value of the occurring corrosion penetration (µm) and p_0^{d}, the design value of the corrosion penetration necessary to produce a crack (µm). Cracking initiation mainly depends on the concrete cover/rebar diameter ratio and the tensile splitting strength of the concrete. Given this relation, parameter p_0^{d} can be calculated by means of Equation 8.

$$p_0^{d} = a_1 + a_2 \cdot \frac{d - \Delta d}{\Phi} + a_3 \cdot f_{c,sp}^{d} \tag{8}$$

With d, the concrete cover (XC3: 35 mm, XS2: 50 mm), Δd, safety margin for the cover thickness (= 14 mm, normal cost of mitigation of risk relative to the cost of repair), Φ, the diameter of the rebar (assumed equal to 12 mm in this case study), a_1, a_2, a_3, three predefined regression parameters and $f_{c,sp}^{d}$, the design value of the tensile splitting strength (MPa). In accordance with DuraCrete, the regression parameters a_1, a_2 and a_3 amounted to 74.4 µm, 7.3 µm and –17.4 µm/MPa, respectively [2].

The occurring corrosion penetration is mainly controlled by the corrosion rate of the reinforcing steel once depassivated. Equation 9 quantifies this parameter.

$$p^d = V^d \cdot w_t \cdot \left(t - t_i^d\right) \tag{9}$$

With V^d, the design value of the corrosion rate (μm/years), w_t, the relative time of wetness (XC3: 0.5, XS2: 1.0), t, the time to unacceptable corrosion-induced cracking (years) and t_i^d, the design value of the time to steel depassivation (years). Although V^d could be measured experimentally, the model relies for its quantification on a pronounced relation between steel corrosion rate and concrete resistivity (Equation 10) as observed by Andrade and Arteaga [8] and supplemented by Nilsson and Gehlen [9].

$$V^d = \frac{m_0}{\rho_0^c \cdot \left(\frac{t_{hydr}}{t_0}\right)^{n_{res}^c} \cdot k_{c,res}^c \cdot \frac{1}{1+K^c\left(T-20\right)} \cdot k_{RH,res}^c \cdot k_{cl,res}^c} \cdot \alpha^c \cdot F_{cl}^c \cdot \gamma_V \tag{10}$$

With m_0, constant for corrosion rate versus resistivity (= 882 μm·Ωm/year), F_{cl}^c, the characteristic value of the chloride corrosion rate factor (XC3: 1.00, XS2: 2.63), α^c, the characteristic value of the pitting factor (XC3: 2.0, XS2: 9.28), γ_V, the partial factor for the corrosion rate (XC3: 1.40, XS2: 1.0), ρ_0^c, the characteristic value of the potential electrolytic resistivity (Ωm), t_0, the age of the concrete at the time of the resistivity measurement (= 28 days or 0.0767 years), t_{hydr}, the age of the concrete corresponding with maximum hydration (= 1 year), n_{res}^c, the age factor for resistivity (OPC concrete: 0.23, FA concrete: 0.62), $k_{c,res}^c$, the characteristic value of the curing factor for the resistivity (= 1.0), $k_{RH,res}^c$, the characteristic value of the humidity factor for the resistivity (XC3: OPC, 80% RH: 3.18, assumed idem for FA and SF concrete, XS2: 1.0), $k_{cl,res}^c$, the characteristic value accounting for the presence of chloride (XC3: 1.0, XS2: 0.72), K^c, characteristic value of the temperature dependency factor (= 0.025°C^{-1} for temperatures below 20°C) and T, the temperature (= 10 °C).

4. LIFE CYCLE ASSESSMENT

In compliance with ISO 14040, the LCA consisted of four major steps: the definition of goal and scope, the inventory analysis, the impact analysis and the interpretation.

4.1 Definition of goal and scope

This LCA was conducted to quantify the theoretical reduction in greenhouse gas emissions that could be achieved by using the proposed HVFA and FA+SF concrete composition instead of traditional OPC concrete. To do this correctly, the LCA study should take into account differences in strength and durability with the latter concrete types. Therefore, the required concrete volume per unit of strength and service life was chosen as functional unit. This was done by dividing the 1 m³ concrete volume by the minimum characteristic cube strength as indicated by the second number in the strength class name (Table 1) and the service life. The value of the functional unit was calculated in two different ways. First of all, it was assumed that service life corresponds with the corrosion initiation period (Table 2, Table 3). Secondly, service life was set equal to the sum of the corrosion initiation period (Table 2, Table 3) and propagation period (Table 4).

4.2 Inventory analysis

Per concrete constituent, the necessary inventory data were collected from the Ecoinvent database [10]. Their proper short descriptions as mentioned in the database are given below.

- Sand 0/4: 'Sand, at mine/CH U'
- Gravel 2/8 and 8/16: 'Gravel, round, at mine/CH U'
- CEM I 52.5 N: 'Portland cement, strength class Z 52.5, at plant/CH U'
- FA: 'Electricity, hard coal, at power plant/BE U', partially by economic allocation
- SF: 'MG-silicon, at plant/NO U', partially by economic allocation

For the allocation of impacts attributed to the industrial by-products FA and SF, the economic allocation coefficients as proposed by Chen et al. [11] and Chen [12] were applied. For the former by-product, this is 1.0% of the impact of the coal fired electricity production corresponding with the production of 1 kg FA. For the latter this is 4.8% of the impact of silicon metal production corresponding with the production of 1 kg SF.

Superplasticizer (SP) inventory data were obtained from an environmental declaration published by the EFCA [13]. The transport of each constituent to the concrete plant was not incorporated in the LCA since its environmental impact is always very case specific. The impacts related with the production process at a concrete plant were included by the partial assignment of the following life cycle inventory (LCI) from Ecoinvent to each concrete composition: 'Concrete, normal at plant/CH U'. It comprises the whole process of producing 1 m³ of ready-mixed concrete, including all internal processes (transport, wastewater treatment, etc.) and infrastructure, and this for a traditional concrete composition which is also accounted for in the LCI. By removing the original concrete constituents and their transport from this inventory, a new LCI is obtained that simply represents the concrete production in general, without any link with a predefined concrete composition. This new LCI was assigned to each of the four studied concrete mixtures.

For all Ecoinvent data, unit processes (U) were used in the modelling of each concrete mixture. This was done to enable a full probabilistic uncertainty analysis of the calculated environmental scores using Monte Carlo. This approach accounts for the small variations in emission values associated with the production of each concrete constituent and enables the calculation of a standard deviation on the concrete's GWP.

4.3 Impact analysis and interpretation

The IPCC 2013 GWP 100a impact method was used to calculate the GWP (kg CO_2 eq) for a timeframe of 100 years. All calculations were done in the LCA software SimaPro 8.

5. RESULTS AND DISCUSSION

5.1 Time to carbonation-induced steel depassivation

Table 2 gives an overview of the estimated characteristic carbonation resistance $R_{0,ca}^{c}$ per concrete mixture. As expected, the concrete mixtures containing large portions of FA (and SF) are much more susceptible to carbonation since part of the $Ca(OH)_2$ produced during cement hydration is being consumed by the pozzolanic reactions that occur. As a consequence, the concrete is characterised by a lower pH value. In comparison with the OPC reference, the carbonation resistance of HVFA composition F50 and FA+SF composition F40SF10 is no less than 72% and 45% lower. This had a significant effect on the estimated duration of the corrosion initiation period t_i^d. While it would take 449.4 years for a rebar present in OPC reference T(0.55) to depassivate, t_i^d would be much shorter for compositions F50 (93.5 years) and F40SF10 (213.2 years).

Table 2: Carbonation resistance and time to carbonation-induced steel depassivation

	T(0.55)	F50	F40SF10
$R_{0,ca}^{c}$ (year · kg/m³/mm²)	2.55×10^{-4}	0.72×10^{-4}	1.40×10^{-4}
t_i^{d} (years)	449.4	93.5	213.2

5.2 Time to chloride-induced steel depassivation

With a value of 4.46×10^{-3} years/mm², the characteristic chloride resistance R_{cl}^{c} of composition F40SF10 surpasses the R_{cl}^{c} value of OPC reference T(0.45) (= 2.97×10^{-3} years/mm²) and the HVFA composition F50 (= 1.97×10^{-3} years/mm²) by far (Table 3).

Table 3: Chloride resistance and time to chloride-induced steel depassivation

	T(0.45)	F50	F40SF10
$R_{Cl,0}^{c}$ ($\times 10^{-3}$ years/mm²)	2.97	1.97	4.46
t_i^{d} (years)	1.7	49.2	77.7

When looking at the estimated time to chloride-induced steel depassivation, the composition with FA and SF looks the most promising. The DuraCrete prediction model indicates that it would take 77.7 years for the steel to depassivate. Surprisingly, this would only take 1.7 years in case of OPC reference T(0.45). Given the fact that the concrete cover was increased from 40 to 50 mm in accordance with Eurocode 2 to achieve an increase in design service life from 50 to 100 years in exposure class XS2, this is a rather striking observation. This very poor service life performance is due to a combination of a low chloride resistance after 28 days and a poor ageing behaviour of the concrete. The age factor n_{Cl}^{c} of submerged OPC concrete should be only 0.3, while values of 0.69 and 0.62 can be assumed for concrete with FA and SF [2]. Previous experimental research done by Van den Heede [1] supports the choice of adopting these clearly different age factors for OPC concrete on the one hand and concrete with FA (and SF) on the other. Age factors derived from chloride migration and diffusion coefficients obtained at different curing ages gave similar results. The excellent ageing behaviour of the HVFA concrete also explains why its depassivation period (= 49.2 years) is longer than for T(0.45) although the former was characterised by a considerably lower chloride resistance R_{Cl}^{c} after 28 days (= 1.97×10^{-3} years/mm² versus 2.97×10^{-3} years/mm²).

5.3 Time to unacceptable corrosion-induced cracking

In terms of decreasing tensile splitting strength (Table 4), the order of mixtures is more less the same as for their compressive strength class (Table 1).

According to Polder, the main influencing factors for resistivity are the moisture content of the concrete (environment) and the concrete composition [14]. Since sample preconditioning should have ensured similar moisture content for all tested mixtures, the observed differences in bulk resistivity must originate from the differences in composition. The lower bulk resistivity of OPC reference T(0.55) (Table 4: 50.02 Ωm) in comparison with T(0.45) (Table 4: 81.49 Ωm) can mainly be explained by the higher W/C ratio of the former mixture (0.55 versus 0.45). A higher W/C ratio normally implies the presence of wider pores. The imposed current will be more easily carried by the ions dissolved in the pore liquid. As a consequence,

the resistivity will be lower [14]. The higher bulk resistivity of the HVFA and FA+SF composition can only in part be explained by their low W/B ratio (0.35). The incorporation of (porosity reducing) reactive minerals such as FA and SF is also known to increase the concrete resistivity [14].

Table 4: Tensile splitting strength, resistivity and time to corrosion-induced cracking

	T(0.55)	T(0.45)	F50	F40SF10
$f_{c,sp}{}^{d}$ (N/mm²)	3.00	4.72	3.55	4.31
$\rho_0{}^{c}$ (Ωm)	50.02	81.49	92.27	352.72
$t_p{}^{d}$ XC3 (years)	31.1	–	141.1	460.8
$t_p{}^{d}$ XS2 (years)	–	0.7	2.5	8.7

The very short propagation period (0.7-8.7 years) after chloride-induced depassivation (Table 4: $t_p{}^{d}$ XS2) is in sharp contrast with the rather long propagation period (31.1-460.8 years) after carbonation-induced depassivation (Table 4: $t_p{}^{d}$ XC3). This can be mainly explained by the higher pitting factor α^{c} (= 9.28 versus 2.0) and corrosion rate factor $F_{cl}{}^{c}$ (= 2.63 versus 1.0) and the lower resistivity chloride factor $k_{cl,res}{}^{c}$ (= 0.72 versus 1.0) that are assumed in environments with presence of chlorides. Since chloride-induced corrosion is known for being very localized and fast, the use of higher values for α^{c} and $F_{cl}{}^{c}$ can be agreed upon intuitively. However, their values could not be verified experimentally until now. This certainly needs to be investigated further on. According to Bertolini et al. [15] though, much longer propagation periods in exposure class XC3 are not so surprising. In structures sheltered from rain, concrete carbonated at the depth of the reinforcement rarely represents any problem in terms of corrosion rate. Because condensation or wetting of the concrete surface only occurs briefly, this will not really lead to an increase in moisture around the reinforcing steel. As a consequence the corrosion rate remains negligible for a longer time. For the submerged exposure condition in marine environments (exposure XS2), one would perhaps also expect that once corrosion initiates, the subsequent propagation phase will be slow due to the very low supply of oxygen. Nonetheless, in Bertolini et al. it is mentioned that presence of defects in the cover of submerged structures may still allow for sufficient oxygen dissolved in the seawater to reach the rebars and consequently sustain significant corrosion [15]. Anyhow, these explanations from literature should still be verified with an experimental determination of the model input parameters that are responsible for the main differences in duration between the carbonation- and chloride induced corrosion propagation periods.

When comparing the corrosion propagation period of the different concrete compositions, it is clear that the presence of supplementary cementitious materials has a very beneficial effect. This is mainly due to their higher resistivity values (Table 4: F50: 92.27 Ωm, F40SF10: 352.72 Ωm) and the excellent ageing behaviour of the alternative binder systems. DuraCrete prescribes an age factor $n_{resR}{}^{c}$ of 0.62 in presence of FA [2]. For a traditional OPC concrete this value amounts to only 0.23. Time dependent monitoring of the concrete resistivity more or less confirmed the prescribed values for the age factors. As such, the propagation period in case of chloride-induced corrosion (exposure class XS2) of compositions F50 and F40SF10 is 1.8 years and 8.0 years longer than for OPC reference T(0.45). In a carbonation exposed environment (exposure classe XC3) with T(0.55) as reference, the corrosion propagation

periods of compositions F50 and F40SF10 increase with no less than 110 years and 429.7 years, respectively.

5.4 Strength and service life related global warming potential

When looking at the required concrete volume per unit of strength and service life (= time to corrosion initiation) in exposure class XC3, it is clear that none of the alternative concrete compositions proposed shows an environmental benefit in comparison with the OPC reference (Figure 1a). If on the other hand the duration of the corrosion propagation period (Table 4: 460.8 years) is included in the calculation of the functional unit for LCA, composition F40SF10 is characterised by a GWP that is 51% lower than the one of OPC reference T(0.55). This approach also reduces the GWP value of HVFA composition F50 a lot as the duration of the corrosion propagation period is substantial (Table 4: 141.1 years). Still, it shows no benefit in comparison with the OPC reference.

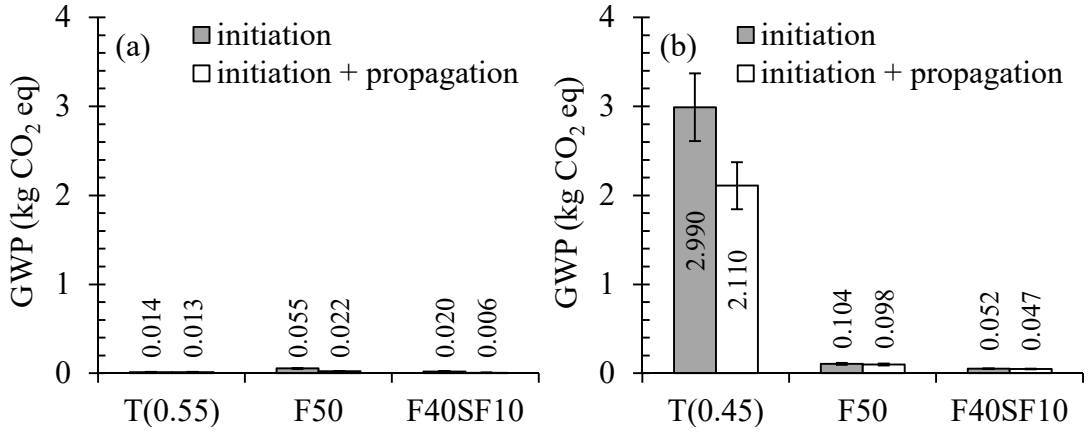

Figure 1: Global warming potential (GWP in kg CO_2 eq) of the required concrete volume per unit of strength and service life in exposure class XC3 (a) and XS2 (b)

Within exposure class XS2 there is already an enormous environmental benefit for HVFA and FA+SF concrete when service life is assumed to correspond with the duration of the corrosion initiation period alone (Figure 1b). In comparison with OPC reference T(0.45), the impact on global warming of compositions F50 and F40SF10 is 97-98% lower. This can mainly be attributed to the very short corrosion initiation period that has been estimated for reference T(0.45) (Table 3: 1.7 years). Additional consideration of the (very short) corrosion propagation periods within the functional unit of all mixtures for exposure class XS2 barely changes the above mentioned possible reduction in GWP.

6. CONCLUSIONS

Within a sheltered carbonation exposed environment (exposure class XC3) it is worthwhile to consider both the corrosion initiation and propagation period to get a proper idea of the concrete's entire service life. On the other hand, the propagation period in submerged marine environments (exposure class XS2) almost turns out negligible in comparison with the initiation period. Thus, only considering the initiation period in DuraCrete does not lead to an important underestimation of the concrete's actual service life. This also means that a strength

and service life related GWP of concrete preferably accounts for both the corrosion initiation and propagation period in environments with exposure to carbonation.

Apart from the experimental input (carbonation resistance, chloride resistance, resistivity, tensile splitting strength), many of the model input parameter values were simply taken from the DuraCrete guideline. Preferably, the validity of each of these prescribed values should be verified experimentally for the specific concrete mixtures under investigation, especially because the corrosion initiation and propagation periods that were estimated now by means of the DuraCrete models sometimes seemed unrealistically long. For the moment, this is still the subject of ongoing research. One of the issues that certainly needs to be dealt with as well is that the models do not account for the almost unavoidable presence of cracks in concrete.

REFERENCES

[1] Van den Heede, P., 'Durability and sustainability of concrete with high volumes of fly ash, PhD thesis (Ghent University, Ghent, 2014).
[2] DuraCrete, 'Probabilistic performance based durability design of concrete structures: General guidelines for durability design and redesign', Document BE95-1347/R15 (CUR, Gouda, 2000).
[3] DuraCrete, 'Probabilistic performance based durability design of concrete structures: Compliance testing for probabilistic design purposes', Document BE95-1347/R8 (CUR, Gouda, 1999).
[4] Sisomphon, K. and Franke, L., 'Carbonation rates of concretes containing high volume of pozzolanic materials', *Cem. Concr. Res.* **37** (12) (2007)1647-1653.
[5] NT Build 492, 'Concrete, mortar and cement-based repair materials: Chloride migration coefficient from non-steady state migration experiments' (Nordtest, Espoo, 1999).
[6] Burden, D., 'The durability of concrete containing high levels of fly ash', PCA R&D Serial No. 2989 (Portland Cement Association, Skokie, 2006).
[7] Weiss, J., Snyder, K., Bullard, J. and Bentz, D., 'Using a saturation function to interpret the electrical properties of partially saturated concrete', *J. Mater. Civ. Eng.* **25** (8) (2013)1097-1106.
[8] Andrade, C. and Arteaga, A., 'Statistical quantification of the propagation period', BE95-134/TG4, Sub-task 4.1 Report (Institute 'Eduardo Torroja' (IET) of Construction Science of the CSIC of Spain, Madrid, 1998).
[9] Nilsson, L.O. and Gehlen, C., 'Summary of the statistical quantification of the DuraCrete resistivity corrosion rate model', BE95-134/TG4, Sub-Task 4.1 Report (Chalmers Univerity of Technology and Institute of Building Research, Technical University of Aachen (ibac), Gothenborg and Aachen, 1998).
[10] Frischknecht, R. and Jungbluth, N. (Eds.), 'Overview and methodology', Final report Ecoinvent v2.0, No. 1 (Swiss Centre for Life Cycle Inventories, St-Gallen, 2007).
[11] Chen, C., Habert, G., Bouzidi, Y., Jullien, A. and Ventura, A., 'LCA allocation procedure used as an incitative method for waste recycling: An application to mineral additions in concrete'. *Resour. Conserv. Recy.* **54** (12) (2010) 1231-1240.
[12] Chen, C., 'A study of traditional and alternative structural concretes by means of the life cycle assessment method', in French, PhD thesis (UTT, Troyes, 2009).
[13] EFCA, European Federation of Concrete Admixtures Associations, 'EFCA environmental declaration superplasticizing admixures (2006) ', EFCA doc 325 ETG [updated 2006 Apr; cited 2013 May 26]. Available from: http://www.efca.info/publications.html.
[14] Polder, R.B., 'Test methods for on site measurement of resistivity of concrete – a RILEM TC-154 technical recommendation', *Constr. Build. Mater.* **15** (2-3) (2001) 125-131.
[15] Bertolini, L., Elsener, B., Pedeferri, P., Redaelli, E. and Polder, R., 'Corrosion of steel in concrete, Prevention, diagnosis, repair', Second, completely revised and enlarged edition (Weinheim: Wiley-VCH Verlag GmbH & Co. KgaA, Weinheim, 2013).